Mutant Phe788 → Leu of the Na^+,K^+-ATPase Is Inhibited by Micromolar Concentrations of Potassium and Exhibits High Na^+-ATPase Activity at Low Sodium Concentrations†

Bente Vilsen*

Department of Physiology, University of Aarhus, Ole Worms Allé 160, DK-8000 Aarhus C, Denmark

Received April 26, 1999; Revised Manuscript Received June 18, 1999

ABSTRACT: Mutant Phe788 → Leu of the rat kidney Na^+,K^+-ATPase was expressed in COS cells to active-site concentrations between 40 and 60 pmol/mg of membrane protein. Analysis of the functional properties showed that the discrimination between Na^+ and K^+ on the two sides of the system is severely impaired in the mutant. Micromolar concentrations of K^+ inhibited ATP hydrolysis ($K_{0.5}$ for inhibition 107 μM for the mutant versus 76 mM for the wild-type at 20 mM Na^+), and at 20 mM K^+, the molecular turnover number for Na^+,K^+-ATPase activity was reduced to 11% that of the wild-type. This inhibition was counteracted by Na^+ in high concentrations, and in the total absence of K^+, the mutant catalyzed Na^+-activated ATP hydrolysis ("Na^+-ATPase activity") at an extraordinary high rate corresponding to 86% of the maximal Na^+,K^+-ATPase activity. The high Na^+-ATPase activity was accounted for by an increased rate of K^+-independent dephosphorylation. Already at 2 mM Na^+, the dephosphorylation rate of the mutant was 8-fold higher than that of the wild-type, and the maximal rate of Na^+-induced dephosphorylation amounted to 61% of the rate of K^+-induced dephosphorylation. The cause of the inhibitory effect of K^+ on ATP hydrolysis in the mutant was an unusual stability of the K^+-occluded $E_2(K_2)$ form. Hence, when $E_2(K_2)$ was formed by K^+ binding to unphosphorylated enzyme, the $K_{0.5}$ for K^+ occlusion was close to 1 μM in the mutant versus 100 μM in the wild-type. In the presence of 100 mM Na^+ to compete with K^+ binding, the $K_{0.5}$ for K^+ occlusion was still 100-fold lower in the mutant than in the wild-type. Moreover, relative to the wild-type, the mutant exhibited a 6−7-fold reduced rate of release of occluded K^+, a 3−4-fold increased apparent K^+ affinity in activation of the *p*NPPase reaction, a 10−11-fold lower apparent ATP affinity in the Na^+,K^+-ATPase assay with 250 μM K^+ present (increased K^+-ATP antagonism), and an 8-fold reduced apparent ouabain affinity (increased K^+-ouabain antagonism).

The Na^+,K^+-ATPase[1] is a transmembrane enzyme responsible for maintaining ionic homeostasis in animal cells by mediating the active extrusion of three Na^+ and uptake of two K^+ for each molecule of ATP being hydrolyzed. As shown in Scheme 1, the ion translocation is linked to ATP hydrolysis through a series of enzyme conformational changes involving at least two interconvertible phosphoenzyme intermediates and two dephosphoenzyme intermediates (*1*−*3*). The phosphorylation of the Na^+,K^+-ATPase by ATP is triggered by the binding to the enzyme of three cytoplasmic sodium ions with high affinity. The phosphoenzyme undergoes a conformational transition from E_1P to E_2P coupled with release of the sodium ions at the extracellular side of the membrane. This is followed by the binding of extracellular K^+ with high affinity, leading to rapid dephosphorylation of E_2P and formation of an intermediate, $E_2(K_2)$, that contains K^+ in an occluded state (*1*). The K^+-occluded $E_2(K_2)$ form can be reached by two different routes: the *physiological* route, just described, and the *direct* route, in which the binding of potassium ions to the E_1

Scheme 1: Minimum Reaction Scheme for the Na^+,K^+-ATPase[a]

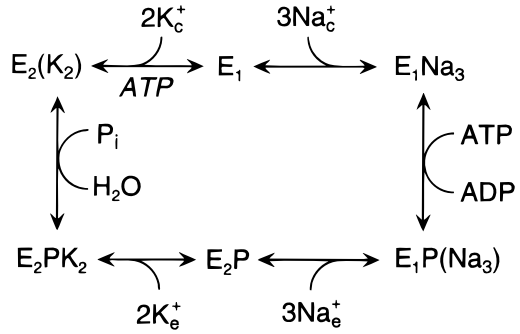

[a] The subscripts c and e indicate the cytoplasmic and extracellular side, respectively. Occluded ions are shown in parentheses. The *ATP* shown in italics indicates the accelerating effect of ATP on the reaction.

† This research was supported by grants from the Danish Medical Research Council, the NOVO Nordisk Foundation, and the Research Foundation of Aarhus University.

* To whom correspondence should be addressed. E-mail: bv@fi.au.dk. Phone: 45 89 42 28 32.

[1] Abbreviations: E_1 and E_2, different conformational states of the Na^+,K^+-ATPase; EP, phosphorylated enzyme; $K_{0.5}$, ligand concentration giving half-maximum activation or inhibition; M1−M10, putative membrane segments numbered from the NH_2-terminal end of the peptide chain; Na^+,K^+-ATPase, the Na^+- and K^+-transporting adenosine triphosphatase (EC 3.6.1.37); *p*NPP, *p*-nitrophenyl phosphate; S1−S5, stalk segments connecting M1−M5 with the cytoplasmic domains; SR Ca^{2+}-ATPase, the sarco(endo)plasmic reticulum Ca^{2+}-transporting adenosine triphosphatase.

10.1021/bi990951t CCC: $18.00
Published on Web 08/13/1999

dephosphoenzyme induces a spontaneous conformational change that occludes the ions (*2*). When the potassium ions bind to E_1 to form $E_2(K_2)$, they act with low affinity at sites facing the inner side of the membrane, and Na^+ competes in rapid equilibrium with K^+ for binding to these sites. Because of the large difference between the apparent Na^+:K^+ affinity ratios on the two sides of the system, the transport normally proceeds in the forward direction with Na^+ being extruded and K^+ being taken up by the cells. The equilibrium distribution between E_1 and E_2 depends on the Na^+:K^+ ratio, pH, and the ATP concentration (*4*). While the rate of the conformational transition from E_2 to E_1 that releases the trapped potassium ions to the interior is very slow in the absence of ATP, 0.1−0.3 s^{-1} at room temperature, the rate of conversion of E_1 to E_2 is rapid, 200−300 s^{-1}. The addition of ATP, which binds at a low-affinity site on $E_2(K_2)$, enhances the rate of K^+ release to 45 s^{-1}. Thus, ATP has a dual role, acting with high affinity it phosphorylates the E_1-Na_3 form of the enzyme, and acting with low affinity and without phosphorylating, it accelerates the change in conformation that releases K^+ to the interior (*1*, *2*, *5*).

It is important to be able to relate the schematic cycle discussed above to the structural elements of the Na^+,K^+-pump. However, the molecular details and spatial organization of the Na^+,K^+-pump are far from being understood. Hence, there are several conspicuous gaps in our knowledge of the pump mechanism; for instance, the nature of the impressive fidelity with which the pump distinguishes between K^+ and Na^+ ions on the two sides of the membrane is virtually unknown and so is the nature of the path taken by the cations through the pump. Information on the molecular details of ion translocation can be obtained using the powerful tool site-directed mutagenesis to pinpoint individual amino acid residues of critical functional importance (*6*−*8*). In fact, data from site-directed mutagenesis analysis of the Na^+,K^+-ATPase and related P-type ATPases such as the SR Ca^{2+}-ATPase and the H^+,K^+-ATPase have focused our attention on the membrane segments M4, M5, and M6 in connection with the binding and occlusion of the transported cations, since mutations to residues with oxygen-containing side chains in these regions were shown to reduce the cation affinities and increase the cation dissociation rates (*6*−*21*). In addition, mutations to Glu781 and Tyr773 in M5, or Asn326 in M4, have been found to impair the discrimination between Na^+ and K^+ (*10*, *21*, *22*).

The central role of M5 in cation translocation is furthermore illustrated by the finding that mutation to the residues equivalent to Glu781 and Tyr773 disturbs the coupling between ATP hydrolysis and cation transport in the H^+-ATPase (*20*) and the SR Ca^{2+}-ATPase (*23*), respectively. Because the conformational changes involved in cation translocation may be expected to require a certain structural flexibility, it is interesting that after tryptic cleavage the M5M6 hairpin region of the Na^+,K^+-ATPase or the H^+,K^+-ATPase can relatively easily be extracted from the membrane (*24*, *25*) and spontaneously leaves the membrane following removal of the occluded cations (*24*, *26*). Moreover, M5 does not appear to act as a full transmembrane insertion sequence by expression in the oocyte system (*27*) and in assays detecting membrane spanning sequences by in vitro translation scanning (*28*−*30*). These findings suggest that the M5M6 hairpin region interacts less with the hydrophobic core of the bilayer and hence is less stably inserted in the membrane as compared with other transmembrane sequences, in accordance with a role as a flexible loop structure that has to move between other membrane segments in connection with ion transport.

The high degree of conservation among Na^+,K^+-, H^+,K^+-, and Ca^{2+}-ATPases of the residues with oxygen-containing side chains in M4, M5, and M6 indicates that other residues (hydrophobic?) must contribute to determine the specific cation selectivities of the P-type pumps. Besides oxygen atoms in the side chains, also aromatic side-chain functions may be of interest in relation to cation binding and selectivity as demonstrated in several studies of ion channel proteins (*31*). Thus, mutagenesis analysis carried out on K^+ channels has revealed an invariant tyrosine, which is critical for K^+ selectivity, located at the entrance to the selectivity filter (*32*, *33*). X-ray analysis of the K^+-channel from *Streptomyces lividans* reveals two layers of aromatic amino acids positioned near the membrane−water interfaces forming a cuff around the selectivity filter thereby holding the pore open at its proper diameter (*34*). Interestingly, several of the transmembrane segments of the Na^+,K^+-ATPase contain aromatic residues near the aqueous boundary, which could serve a similar role as in the K^+-channels with selectivity being based on the difference between the ionic radii of Na^+ and K^+.

The present investigation has been undertaken to elucidate the functional role of the phenylalanine Phe788 located in M5 of the rat kidney Na^+,K^+-ATPase.[2] This phenylalanine is well conserved among most Na^+,K^+-ATPases and is conservatively replaced by tyrosine in some Na^+,K^+-ATPases and in H^+,K^+-ATPases, whereas it is replaced by either threonine, serine, alanine, or glycine in the various classes of Ca^{2+}-ATPases and by leucine or isoleucine in fungal H^+-ATPases (*35*, *36*). In this study, Phe788 was replaced by leucine to remove the aromatic ring structure while retaining some of the bulk and hydrophobicity of the side chain. The Phe788 → Leu mutant exhibited a high Na^+-activated ATPase activity in the absence of K^+ and an unusual stabilization of the $E_2(K_2)$ intermediate, resulting in K^+ inhibition of the ATPase activity. These effects of the mutation severely impair the discrimination between Na^+ and K^+ on the two sides of the system.

MATERIALS AND METHODS

Oligonucleotide-directed mutagenesis of the cDNA encoding the ouabain-insensitive rat α1-isoform of the Na^+,K^+-ATPase, the expression of the mutant and wild-type in COS-1 cells by selection of stable transfectants in 5 μM ouabain, membrane preparation, protein determination, measurement of the rate of ATP hydrolysis, and assays for phosphorylation and dephosphorylation kinetics were carried out as previously described (*10*, *37*). The oligonucleotide used for introduction of the Phe788 → Leu mutation was TTCTTGATAC*TG*ATTATTGCA, where the asterisks mark the bases which have been altered relative to wild-type. The molecular rate of ATP hydrolysis ("turnover number"), in $minutes^{-1}$, was calculated as the ratio between

[2] The phenylalanine residue Phe788 of the rat α1-isoform of the Na^+,K^+-ATPase is examined in the present study. The equivalent residue of the sheep isoform is Phe786.

the ATPase activity and the active-site concentration determined as the maximum amount of phosphoenzyme formed in the presence of oligomycin (*37*). Deocclusion of K^+ was studied at 10 °C as described in ref *11*, except that in some experiments 100 mM Na^+ was present during the equilibration with K^+ as described in the figure legend. In all the above-mentioned functional assays, ouabain (10 or 20 μM, see figure legends) was included to inhibit the endogenous enzyme.

p-Nitrophenyl phosphatase (*p*NPPase) was assayed by incubating deoxycholate-treated leaky membranes for 5−18 min at 37 °C in the presence of 30 mM histidine, (pH 7.4), 10 mM $MgCl_2$, 10 mM *p*NPP (Tris salt), 0.2 mM EGTA, and the indicated concentrations of KCl (or without KCl for determination of background), essentially as described in ref *38*. Formation of *p*-nitrophenol was measured by reading the absorbance at 410 nm. The specific K^+-*p*NPPase activity was calculated from the difference between values measured with and without K^+. The rate of *p*NPP hydrolysis was found to be constant over the incubation time at all the K^+ concentrations tested.

RESULTS

Expression. The mammalian COS cell system was used to express the wild-type and mutant Phe788 → Leu of the rat kidney Na^+,K^+-ATPase. The expression strategy used takes advantage of the well-established difference between the ouabain sensitivities of the exogenous rat Na^+,K^+-ATPase and the Na^+,K^+-ATPase present endogenously in the COS cells, allowing transfected cells expressing functional rat Na^+,K^+-ATPase to be isolated in the presence of ouabain, due to preferential inhibition of the endogenous enzyme, as previously described (*10*, *11*, *37*). The cells expressing the exogenous rat wild-type were grown at a low K^+ concentration (0.9 mM) to upregulate the expression to the highest possible level as described in ref *10*. For the mutant enzyme, on the other hand, the maximal expression level was achieved at 2−5 mM extracellular K^+. Under these conditions, the wild-type and mutant enzymes were expressed to site concentrations between 40 and 60 pmol/mg of membrane protein, corresponding to 85−90% of the Na^+,K^+-ATPase molecules present in the respective membrane preparations, and the endogenous ouabain-sensitive Na^+,K^+-ATPase contributed only 10−15% of the molecules. These numbers are based on the capacity for oligomycin-supported phosphorylation from ATP determined with and without preincubation with ouabain. The ability of mutant Phe788 → Leu to confer ouabain resistance to the COS cells demonstrated that at this high level of expression the rates of Na^+ and K^+ transport catalyzed by the mutant are compatible with cell growth.

Na^+ Dependence of Na^+,K^+-ATPase Activity. Figure 1 presents the results of experiments in which the Na^+ concentration dependence of the molecular rate of ATP hydrolysis (turnover number) of the Phe788 → Leu mutant and the wild-type Na^+,K^+-ATPase was determined in the presence of 3 mM ATP at three different K^+ concentrations, 250 μM, 2 mM, and 20 mM, as well as in absence of K^+ (Na^+-ATPase activity). The measurements were carried out in the presence of 10 μM ouabain to inhibit the endogenous Na^+,K^+-ATPase (cf. Figure 9). For the wild-type enzyme

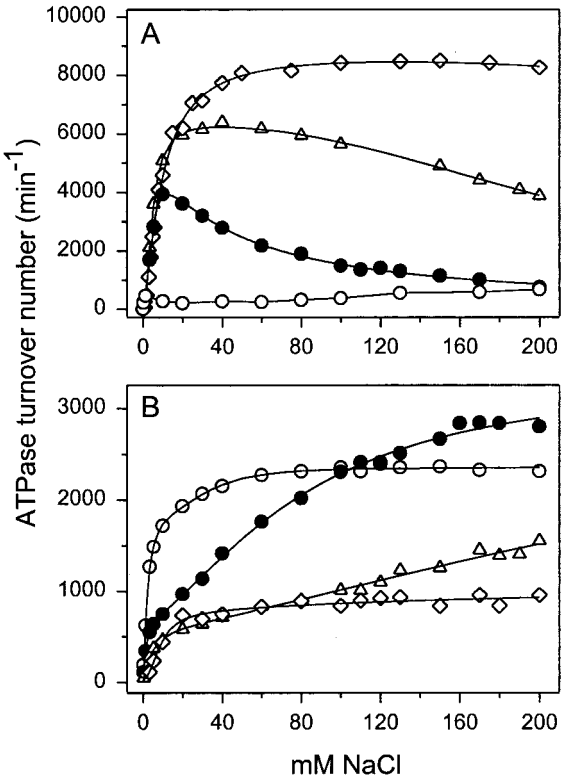

FIGURE 1: Na^+ dependence of the molecular rate of ATP hydrolysis ("turnover number") of wild-type Na^+,K^+-ATPase (A) and the Phe788 → Leu mutant (B) measured at 37 °C in the presence of 3 mM ATP, 3 mM $MgCl_2$, 30 mM histidine buffer (pH 7.4), 1 mM EGTA, 10 μM ouabain, the indicated NaCl concentrations, and KCl concentrations as follows: (○) absence of added KCl; (●) 250 μM KCl; (△) 2 mM KCl; (◇) 20 mM KCl. The Na^+-ATPase data (○) in panel A were transferred from Figure 3 in ref *10*. For the other conditions, the data points (average values corresponding to three experiments) were fitted to the sum of two components: $V = a_1[Na^+]^n/[(K_1)^n + [Na^+]^n] \pm a_2[Na^+]^m/[(K_2)^m + [Na^+]^m)]$ where the minus sign applies to the inhibitory phases in panel A. In each case, the line shows the best fit. The following values were obtained for the Na^+ concentrations giving half-maximum activation and inhibition. (A) (●) $K_1 = 4.53$ mM, $K_2 = 35.0$ mM; (△) $K_1 = 4.87$ mM, $K_2 = 222$ mM; (◇) $K_1 = 9.72$ mM, $K_2 = 681$ mM. (B) (○) $K_1 = 2.26$ mM, $K_2 = 33.5$ mM; (●) $K_1 = 2.50$ mM, $K_2 = 81.7$ mM; (△) $K_1 = 4.43$ mM, $K_2 = 319$ mM; (◇) $K_1 = 8.96$ mM, $K_2 = 28\,902$ mM. The following amplitudes were obtained for the two activating phases in panel B: (○) $a_1 = 1940$ min^{-1}, $a_2 = 420$ min^{-1}; (●) $a_1 = 902$ min^{-1}, $a_2 = 2397$ min^{-1}; (△) $a_1 = 634$ min^{-1}, $a_2 = 2702$ min^{-1}; (◇) $a_1 = 641$ min^{-1}, $a_2 = 2419$ min^{-1}.

(Figure 1A), the maximum activity increases with increasing K^+ concentration. At all three K^+ concentrations, Na^+ in low concentration activates ATP hydrolysis ($K_{0.5}$ values in the range 4−10 mM), whereas high concentrations of Na^+ inhibit ($K_{0.5}$ values in the range 35−681 mM, see figure legend). The efficiency of this Na^+ inhibition increases with decreasing K^+ concentration, being most prominent at 250 μM K^+. Such a pattern of activation followed by inhibition is in accordance with the literature (*39*). The activation by low Na^+ concentrations reflects the stimulation of phosphorylation by Na^+ binding at cytoplasmically facing (internal) high-affinity sites. The inhibitory phase of the curves reflects inhibition of dephosphorylation of the E_2P phosphoenzyme intermediate by Na^+ binding in competition with K^+ at the extracellularly facing (external) sites. Although Na^+ can bind at these sites and induce dephosphorylation, Na^+ is a poor substitute for K^+ in the wild-type enzyme, and the Na^+-

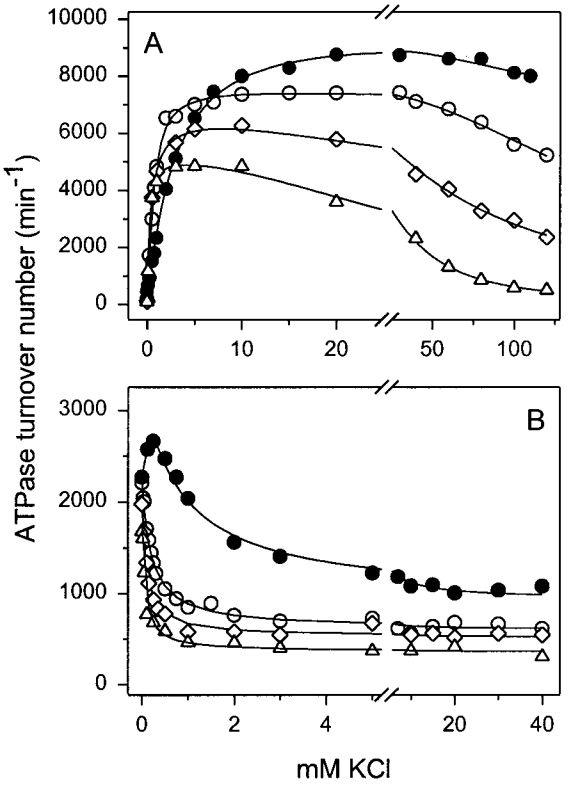

FIGURE 2: K^+ dependence of the molecular rate of ATP hydrolysis ("turnover number") of wild-type Na^+,K^+-ATPase (A) and the Phe788 → Leu mutant (B) measured at 37 °C in the presence of 3 mM ATP, 3 mM $MgCl_2$, 30 mM histidine buffer (pH 7.4), 1 mM EGTA, 10 μM ouabain, the indicated KCl concentrations, and NaCl concentrations as follows: (△) 10 mM NaCl; (◇) 20 mM NaCl; (○) 40 mM NaCl; (●) 200 mM NaCl. In panel A the data points (average values corresponding to three experiments) were fitted to the following function: $V = a_1[K^+]^n/[(K_1)^n + [K^+]^n] - a_2[K^+]^m/[(K_2)^m + [K^+]^m]$ where the minus sign corresponds to the inhibitory phase. In each case, the line shows the best fit. The following values were obtained for the K^+ concentrations giving half-maximum activation (K_1) and inhibition (K_2): (△) K_1 = 0.244 mM, K_2 = 34.4 mM; (◇) K_1 = 0.430 mM, K_2 = 76.3 mM; (○) K_1 = 0.650 mM, K_2 = 178 mM; (●) K_1 = 3.20 mM, K_2 = 444 mM. In panel B, the data points (average values corresponding to three experiments) were fitted to the following function: $V = V_{max} - a[K^+]^n/[(K_{0.5})^n + [K^+]^n]$, excluding the two data points corresponding to KCl concentrations lower than 0.25 mM at 200 mM NaCl (the small activating phase) from the fitting procedure. The following values were obtained for the K^+ concentrations giving half-maximum inhibition ($K_{0.5}$): (△) 0.072 mM; (◇) 0.107 mM; (○) 0.203 mM; (●) 0.847 mM.

induced dephosphorylation is rather slow compared with the K^+-induced dephosphorylation (see below).

The corresponding curves for the Phe788 → Leu mutant (Figure 1B) have a totally different appearance. First, increasing concentrations of K^+ inhibit enzyme activity contrary to the situation with the wild-type enzyme. Thus, the maximal Na^+,K^+-ATPase activity of the mutant is observed in the presence of 250 μM K^+ and the minimal Na^+,K^+-ATPase activity at 20 mM K^+. Even the maximum turnover number reached at 250 μM K^+ in the mutant (approximately 2800 min^{-1}) is severely reduced relative to the maximum turnover number of the wild-type (approximately 8500 min^{-1}).

Second, in the presence of K^+, the activation of the mutant ATPase activity by Na^+ follows an unusual biphasic pattern with high-affinity and low-affinity activation phases, the latter

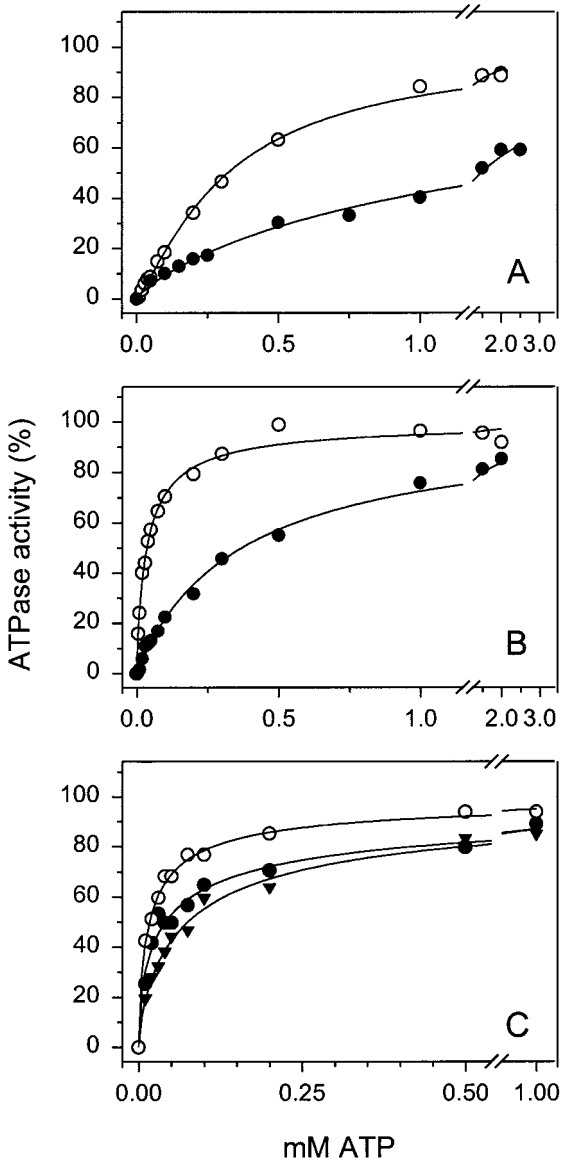

FIGURE 3: ATP dependence of the rate of ATP hydrolysis of wild-type Na^+,K^+-ATPase (○) and the Phe788 → Leu mutant (●, ▼) measured at 37 °C in the presence of 3 mM $MgCl_2$, 30 mM histidine buffer (pH 7.4), 1 mM EGTA, 10 μM ouabain, and the following NaCl and KCl concentrations: (A) 130 mM NaCl and 20 mM KCl; (B) 130 mM NaCl and 250 μM KCl; (C) 200 mM (○, ●) or 20 mM (▼) NaCl and no added KCl. The data points (average values corresponding to 2−3 experiments) were fitted to the following function: $V = V_{max}[ATP]^n/[(K_{0.5})^n + [ATP]^n]$. In each case, the line shows the best fit with V_{max} normalized to 100%. The following values were obtained for the ATP concentrations giving half-maximum activation ($K_{0.5}$). (A) (○) 0.321 mM; (●) 1.46 mM. (B) (○) 0.036 mM; (●) 0.369 mM. (C) (○) 0.016 mM; (●) 0.041 mM; (▼) 0.075 mM.

appearing most prominently in the curves for 250 μM K^+ and 2 mM K^+. The apparent affinities for Na^+ activation corresponding to the high-affinity phase are very similar to those obtained for the wild-type (compare the $K_{0.5}$ values 2.5, 4.43, and 8.96 mM with the values for the wild-type, 4.53, 4.87, and 9.72 mM, corresponding to 250 μM, 2 mM, and 20 mM K^+, respectively), suggesting that the intracellularly facing Na^+ sites are functioning normally in the mutant. The apparent affinities corresponding to the unusual Na^+ activation with low affinity fall within the range of Na^+ concentrations that inhibit ATP hydrolysis in the wild-type

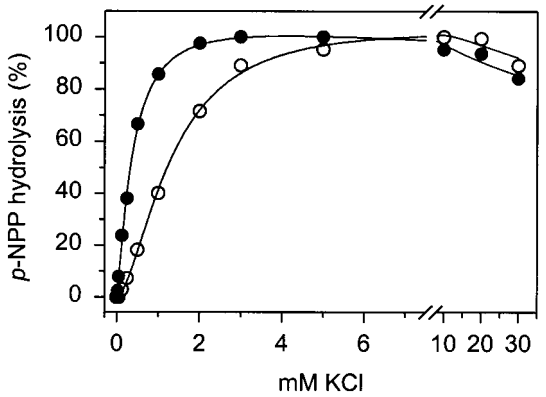

FIGURE 4: K^+ dependence of the *p*NPPase activity of wild-type Na^+,K^+-ATPase (○) and the Phe788 → Leu mutant (●). The measurement was carried out as described in the Materials and Methods at 37 °C in the presence of 10 mM *p*NPP, 10 mM Mg^{2+}, 30 mM histidine buffer (pH 7.4), 0.2 mM EGTA, and the indicated concentrations of KCl. The data points are average values corresponding to 2 experiments. The K^+ concentrations giving half-maximum activation are 1.36 mM (○) and 0.379 mM (●).

enzyme (compare the $K_{0.5}$ values of 82 mM and 35 mM determined for the mutant and wild-type, respectively, at 250 μM K^+, and the $K_{0.5}$ values of 319 and 222 mM for the mutant and wild-type, respectively, at 2 mM K^+).

Third, in the total absence of K^+, the Na^+ activation curves differ conspicuously between wild-type and mutant. Surprisingly, the mere presence of Na^+ activates the rate of ATP hydrolysis of the mutant to a level 3−4-fold higher than that seen for the wild-type under similar conditions (compare 2400 min^{-1} for the mutant with 670 min^{-1} for the wild-type, at 200 mM Na^+). In the mutant, the maximum level of Na^+-ATPase activity of 2400 min^{-1} amounts to as much as 86% of the maximum level of Na^+,K^+-ATPase activity (observed in the presence of 250 μM K^+), whereas in the wild-type, the maximal Na^+-ATPase activity corresponds to 7.9% of the maximal Na^+,K^+-ATPase activity. It is furthermore notable that the major part (approximately 82%) of the mutant Na^+-ATPase activity is activated by Na^+ binding with high affinity ($K_{0.5}$ 2.3 mM) and only a minor part of the activation seems to require Na^+ binding with lower affinity ($K_{0.5}$ 34 mM). The wild-type Na^+-ATPase activity, by contrast, shows a complex activation pattern with a small activation at low Na^+ concentrations, due to Na^+ binding at the internal sites, being followed by a combination of inhibition and activation at higher Na^+ concentrations, due to Na^+ binding at inhibitory as well as the activating extracellularly facing sites as previously discussed (*10*). The $K_{0.5}$ for the activating effect of Na^+ on the external sites of the wild-type is higher than 100 mM. The $K_{0.5}$ of 2.3 mM for Na^+ activation of the major part of the Na^+-ATPase activity in the mutant is similar to the $K_{0.5}$ for Na^+ activation of phosphorylation from ATP in the mutant (2.5 mM, data not shown), and these $K_{0.5}$ values are only about 3-fold higher than the $K_{0.5}$ for Na^+ activation of phosphorylation from ATP in the wild-type (0.7−0.8 mM, cf. refs *10* and *37*). This supports the notion that the intracellularly facing high-affinity activating Na^+ sites are little disrupted by the mutation and suggests that either the external activating sites have acquired much higher affinity for Na^+ in the mutant relative to the wild-type, or the major part of the activation occurs without any requirement for Na^+ at external sites.

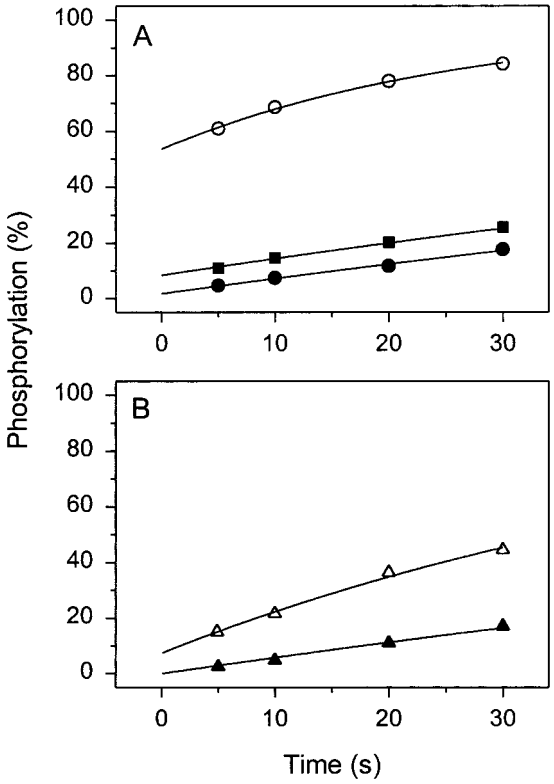

FIGURE 5: Time course of phosphorylation with [γ-^{32}P]ATP of the wild-type Na^+,K^+-ATPase (○, △) and the Phe788 → Leu mutant (●, ■, ▲) at 10 °C in the presence of 100 mM NaCl following incubation with various concentrations of KCl in the absence of Na^+. Deoxycholate treated microsomes were first incubated at 37 °C for 10 min in 20 μM ouabain, 3 mM $MgCl_2$, and 20 mM Tris buffer (pH 7.5). This was followed by incubation at room temperature for 1 h with 10 μM (■), 100 μM (○, ●), or 1 mM (△, ▲) KCl. At the end of the incubation at room temperature, oligomycin was added at a concentration of 150 μg/mL, and 1 min later the sample, comprising 41 μL, was cooled to 10 °C. Deocclusion of K^+ and phosphorylation of the deoccluded enzyme were initiated by addition of 360 μL of a phosphorylation solution (of the same temperature) to produce final concentrations of 100 mM NaCl, 1 μM [γ-^{32}P]ATP, 1 mM $MgCl_2$, 1 mM EGTA, 20 mM Tris buffer (pH 7.5), and dilute the K^+ concentration to one-tenth that originally present during the 1 h incubation. Acid quenching of the phosphoenzyme was performed at the indicated time intervals following the initiation of deocclusion. For determination of maximum phosphorylation (representing fully deoccluded enzyme), the 1 h incubation was carried out in the presence of 50 mM NaCl and absence of K^+. The background phosphorylation determined in the presence of 50 mM KCl without Na^+ (less than 10% of maximum phosphorylation) was subtracted and the resulting data points (average values corresponding to two to five experiments) were fitted to a biphasic time course as previously described (*11*). The curves show the fits corresponding to times ≥5 s, i.e., the slow phases corresponding to deocclusion of K^+. The amplitudes and extracted rate constants corresponding to the slow phase are as follows: (panel A) (○) 46.4%, 0.0368 s^{-1}; (●) 98.3%, 0.0057 s^{-1}; (■) 91.6%, 0.0068 s^{-1}; (panel B) (△) 92.7%, 0.0176 s^{-1}; (▲) 100%, 0.0060 s^{-1}.

K^+ Dependence of Na^+,K^+-ATPase Activity. Figure 2 presents the results of a series of experiments in which the K^+ concentration dependence of the turnover number for ATP hydrolysis was determined in the presence of 3 mM ATP at four different Na^+ concentrations. Overall, the curves for the wild-type enzyme (Figure 2A) follow a pattern with the enzyme being activated by low K^+ concentrations and inhibited by high K^+ concentrations. The activation phase, reflecting stimulation of dephosphorylation by K^+ binding

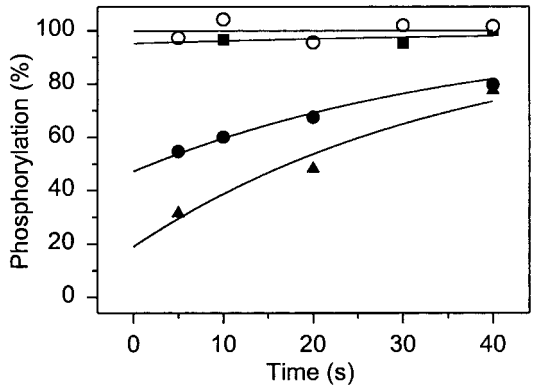

FIGURE 6: Time course of phosphorylation with [γ-^{32}P]ATP of the wild-type Na^+,K^+-ATPase (○) and the Phe788 → Leu mutant (●, ■, ▲) at 10 °C in the presence of 100 mM NaCl following incubation with various concentrations of KCl in the presence of 100 mM NaCl. Except for the presence of 100 mM NaCl during the 1 h incubation with 10 μM (■), 100 μM (○, ●), or 1 mM (▲) KCl, the experiments were carried out and analyzed as described for Figure 5. The amplitudes and extracted rate constants corresponding to the slow phase are as follows: (○) 0%; (●) 52.9%, 0.0268 s^{-1}; (■) 4.7%, 0.0226 s^{-1}; (▲) 81.1%, 0.0279 s^{-1}.

at the extracellularly facing uptake sites, corresponds to $K_{0.5}$ values of 0.244, 0.430, 0.650 mM, and 3.2 mM at 10, 20, 40, and 200 mM Na^+, respectively, in accordance with a competition between Na^+ and K^+ at these sites (*3*). The inhibition phase, reflecting inhibition of phosphorylation by K^+ binding in competition with Na^+ at the internal high-affinity Na^+ sites, corresponds to apparent $K_{0.5}$ values for inhibition of enzyme activity of 34, 76, 178, and 444 mM at 10, 20, 40, and 200 mM Na^+, respectively.

Again, the corresponding curves obtained with the Phe788 → Leu mutant (Figure 2B) are very different from those of the wild-type. At 10, 20, and 40 mM Na^+, maximal activation is reached below 200 μM K^+. Only the curve representing the experiments carried out at 200 mM Na^+ shows a rudimentary activation phase with maximum activity being reached at 250 μM K^+ in accordance with the finding in Figure 1B. Relative to the wild-type, the inhibition by K^+ in the mutant occurs at extremely low K^+ concentrations, the $K_{0.5}$ values for K^+ inhibition being 72, 107, 203, and 847 μM in the presence of 10, 20, 40, and 200 mM Na^+, respectively. Thus, the apparent affinities with which K^+ exerts its inhibitory effect in the mutant correspond much better to the apparent affinities for K^+ activation in the wild-type than to the apparent affinities for K^+ inhibition in the wild-type, suggesting that the inhibition in the mutant might be due to K^+ binding at the extracellularly facing uptake sites (*1*).

ATP Dependence of ATPase Activity. The ATP dependence of the ATPase activity was analyzed at various K^+ and Na^+ concentrations for the Phe788 → Leu mutant and the wild-type Na^+,K^+-ATPase, and Figure 3 shows the ATPase activities expressed as percentages of the extrapolated values corresponding to infinite ATP concentration. The experiments corresponding to Figure 3, panels A and B, were carried out in the presence of 130 mM Na^+ with either 20 mM K^+ or 250 μM K^+, respectively. In the presence of 20 mM K^+, the mutant displayed a 4−5-fold reduced apparent affinity for ATP relative to the wild-type enzyme (compare the $K_{0.5}$ value of 0.321 mM for the wild-type with that of 1.46 mM for the mutant). When the concentration of K^+ was reduced to 250 μM, i.e., the concentration giving maximal Na^+,K^+-ATPase activity in the mutant according to Figures 1B and 2B, the apparent ATP affinity increased in both the mutant and the wild-type, but less so in the mutant. Thus, at 250 μM K^+, the mutant displayed a 10−11-fold lower apparent ATP affinity compared with the wild-type ($K_{0.5}$ values of 0.036 and 0.369 mM for the wild-type and the mutant, respectively). The apparent affinities for ATP determined in the Na^+-ATPase assay in the absence of K^+ (Figure 3C) were higher and differed less between wild-type and mutant ($K_{0.5}$ values of 0.016 and 0.041 mM, respectively, at 200 mM Na^+, and 0.075 mM for the mutant at 20 mM Na^+).

In the wild-type Na^+,K^+-ATPase, the E_1Na_3 form, which is phosphorylated by ATP, possesses very high affinity for ATP corresponding to a dissociation constant in the submi-

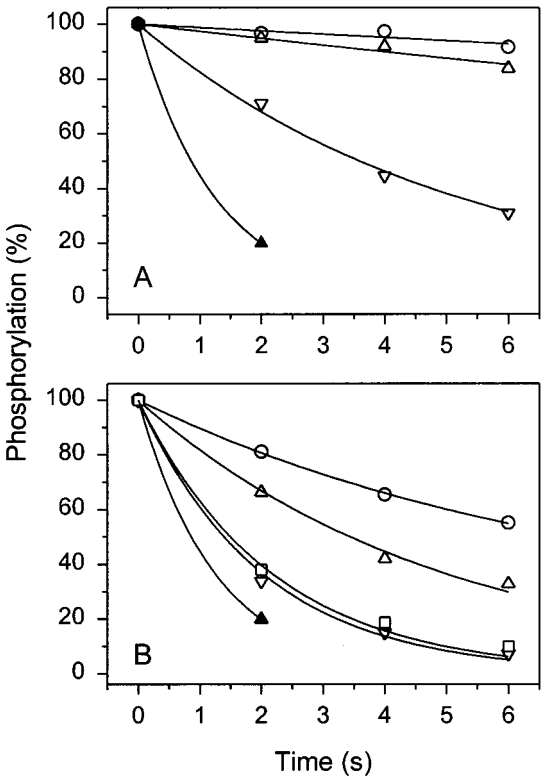

FIGURE 7: Na^+ dependence of dephosphorylation of the wild-type Na^+,K^+-ATPase (A) and the Phe788 → Leu mutant (B). Following preincubation of the deoxycholate treated microsomes at 37 °C for 10 min in 20 μM ouabain, 3 mM $MgCl_2$, and 20 mM Tris buffer (pH 7.5), the phosphoenzyme was formed at 0 °C in a 15 s reaction with 2 μM [γ-^{32}P]ATP in the presence of 20 mM NaCl, 130 mM choline chloride, 3 mM $MgCl_2$, 20 mM Tris buffer (pH 7.4), 1 mM EGTA, and 20 μM ouabain. The phosphoenzyme was either acid quenched directly after the 15 s reaction ("0 s" point) or was diluted 10-fold in ice-cold medium of the same composition except for the absence of [γ-^{32}P]ATP and the presence of 1.1 mM unlabeled ATP and varying concentrations of NaCl, KCl, and choline chloride to produce the following final concentrations: (○) 2 mM NaCl, 0 mM KCl, 148 mM choline chloride; (△) 20 mM NaCl, 0 mM KCl, 130 mM choline chloride; (▽) 137 mM NaCl, 0 mM KCl, 13 mM choline chloride; (□) 200 mM NaCl, 0 mM KCl, 0 mM choline chloride; (▲) 20 mM NaCl, 20 mM KCl, 110 mM choline chloride. Acid quenching was performed at the indicated time intervals following the dilution. The data points (average values corresponding to two to four experiments) were fitted to monoexponential decays giving the following rate constants. (A) (○) 0.0124 s^{-1}; (△) 0.0266 s^{-1}; (▽) 0.193 s^{-1}; (▲) 0.800 s^{-1}. (B) (○) 0.102 s^{-1}; (△) 0.202 s^{-1}; (▽) 0.497 s^{-1}; (□) 0.463 s^{-1}; (▲) 0.81 s^{-1}.

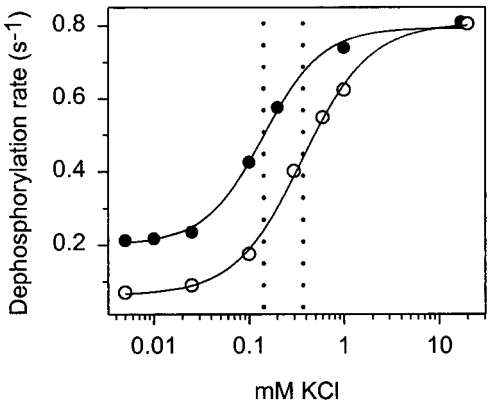

FIGURE 8: K^+ dependence of dephosphorylation of the wild-type Na^+,K^+-ATPase (○) and the Phe788 → Leu mutant (●). Following preincubation of the deoxycholate treated microsomes at 37 °C for 10 min in 20 μM ouabain, 3 mM $MgCl_2$, and 20 mM Tris buffer (pH 7.5) the phosphoenzyme was formed at 0 °C in a 15 s reaction with 2 μM [γ-^{32}P]ATP in the presence of 20 mM NaCl, 130 mM choline chloride, 3 mM $MgCl_2$, 20 mM Tris buffer (pH 7.4), 1 mM EGTA, and 20 μM ouabain. The phosphoenzyme was either acid quenched directly after the 15 s reaction ("0 s" point) or was diluted 10-fold in ice-cold medium of the same composition except for the absence of [γ-^{32}P]ATP and the presence of 1.1 mM unlabeled ATP and varying concentrations of choline chloride and KCl and to produce the indicated final concentrations of KCl with [KCl] + [choline chloride] = 130 mM. Acid quenching was then performed 2 s later and the ordinate shows the rate constants for the dephosphorylation occurring within the 2 s chase period. The data points (average values corresponding to three or four experiments) were fitted to the Hill equation with an offset representing dephosphorylation in the absence of K^+, giving $K_{0.5}$ values of 0.37 and 0.14 mM (indicated by dotted lines) and V_{max} values of 0.81 and 0.79 s^{-1} for the wild-type and the mutant, respectively.

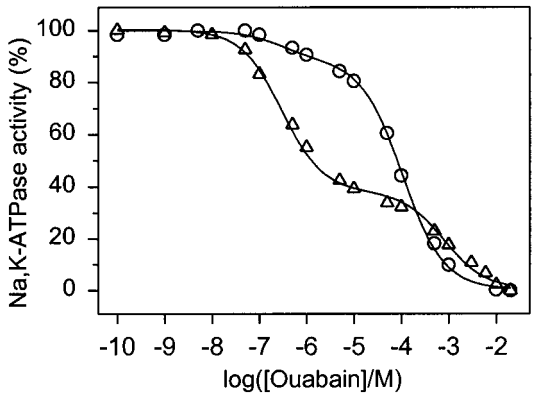

FIGURE 9: Ouabain sensitivity of Na^+,K^+-ATPase activity of plasma membranes isolated from COS-1 cells expressing the wild-type rat kidney enzyme (○) or the Phe788 → Leu mutant (△). The rate of ATP hydrolysis was determined at 37 °C in the presence of 130 mM NaCl, 20 mM KCl, 3 mM ATP, 3 mM $MgCl_2$, 30 mM histidine buffer (pH 7.4), 1 mM EGTA, and the indicated concentrations of ouabain. The data points (average values corresponding to two experiments) were fitted to a function with the ouabain-inhibited enzyme represented by the sum of two hyperbolic components: $V = V_{max} - [a_1[\text{ouabain}]/(K_1 + [\text{ouabain}]) + a_2[\text{ouabain}]/(K_2+[\text{ouabain}])]$. In each case, the line shows the best fit with V_{max} normalized to 100%. The following values were obtained for the contributions of the endogenous enzyme and the expressed exogenous enzyme to the ATPase activity (a_1 and a_2, respectively) and the respective inhibition constants (K_1 and K_2, respectively). Wild-type: $a_1 = 11.5\%$, $a_2 = 88.0\%$, $K_1 = 0.3$ μM, $K_2 = 106$ μM. Mutant: $a_1 = 62.3\%$, $a_2 = 37.7\%$, $K_1 = 0.3$ μM, $K_2 = 807$ μM.

cromolar range, but ATP bound to the $E_2(K_2)$ form with low affinity (dissociation constant in the millimolar range) accelerates the $E_2(K_2)$ to E_1Na_3 conformational transition, which is rate limiting for the overall ATP hydrolysis reaction (*1*, *5*). The apparent affinity determined by titration of the ATP dependence of the Na^+,K^+-ATPase activity therefore reflects the steady-state distribution of low-affinity $E_2(K_2)$ and high-affinity E_1Na_3 forms. This explains the large shift toward a higher apparent ATP affinity observed in the wild-type when the steady-state concentration of the $E_2(K_2)$ form is lowered by reducing the K^+ concentration from 20 mM to 250 μM K^+ (K^+-ATP antagonism). The lower apparent ATP affinity observed for the mutant at 250 μM K suggests that $E_2(K_2)$ accumulates at a lower K^+ concentration in the Phe788 → Leu mutant relative to the wild-type.

Effects of K^+ on pNPPase Activity. The wild-type Na^+,K^+-ATPase is able to catalyze a Mg^{2+}-dependent, K^+-activated hydrolysis of the substrate *p*-nitrophenyl phosphate (*p*NPP). The mechanism of the K^+-activated hydrolysis of *p*NPP is not well understood, but it has been suggested that it occurs without formation of a phosphorylated intermediate and that it is the $E_2(K_2)$ form of the dephosphoenzyme that is responsible for the phosphatase activity (*3*, *40*).

The K^+ dependence of the *p*NPPase activity at 10 mM *p*NPP and 10 mM Mg^{2+} was measured on the membranes containing the expressed wild-type Na^+,K^+-ATPase or the Phe788 → Leu mutant, and the results corrected for the activity found in the presence of Mg^{2+} without added K^+ are shown in Figure 4. The measured activity represents not only the activity contributed by the wild-type or the Phe788 → Leu mutant but includes in addition the activity contributed by the endogenous COS cell Na^+,K^+-ATPase. This is because the activity was measured in the absence of ouabain which is less efficient as inhibitor of the phosphatase activity as compared with the Na^+,K^+-ATPase activity. Anyway, it is possible to compare wild-type and mutant *p*NPPase activities, because the endogenous COS cell enzyme contributes as little as 12−15% of the Na^+,K^+-ATPase molecules present (see above and Figure 9). In the wild-type Na^+,K^+-ATPase as well as the Phe788 → Leu mutant, the rate of *p*NPP hydrolysis increases to a maximum and decreases above 10 mM K^+, probably due to an inhibitory effect of ionic strength (*41*). The maximum turnover numbers calculated after correction for the *p*NPPase activity contributed by the endogenous enzyme were 2488 and 2002 min^{-1} for the wild-type and the mutant, respectively. The response of the *p*NPPase activity to varying K^+ concentration indicates a $K_{0.5}$ for K^+ activation of 1.36 mM for the wild-type enzyme in accordance with the values in the literature (*42*). The Phe788 → Leu mutant, on the other hand, exhibited a $K_{0.5}$ of 0.379 mM corresponding to a 3−4-fold increase in apparent affinity relative to the wild-type enzyme in accordance with a stabilization of the $E_2(K_2)$ form in the mutant.

K^+ Occlusion. To examine the hypothesis that the K^+ occluded $E_2(K_2)$ form is more stable in the Phe788 → Leu mutant than in the wild-type Na^+,K^+-ATPase, the method originally described by Blostein and co-workers (*43*) and later adapted by Vilsen and Andersen (*11*) was applied. In short, $E_2(K_2)$ is formed by equilibrating the enzyme with K^+ in the absence of Na^+ and ATP. At the end of the equilibration period, oligomycin is added and the time course of phosphoenzyme formation is monitored upon a 10-fold dilution of the enzyme in a solution containing the substrates

[γ-^{32}P]ATP and Na^+ required for phosphorylation. The addition of oligomycin ensures rapid phosphorylation of the E_1Na_3 form and stabilization of the phosphoenzyme. Under these conditions, the phosphorylation of enzyme present in the occluded $E_2(K_2)$ form proceeds through the steps $E_2(K_2) \rightarrow E_1 \rightarrow E_1P(Na_3)$ with the release of occluded K^+ being rate limiting. On the other hand, enzyme without occluded K^+ binds Na^+ instantaneously and phosphorylates within the first 5 s after addition of ATP.

Figure 5 present results of such experiments with the wild-type and the Phe788 → Leu mutant equilibrated with K^+ concentrations of 10 μM, 100 μM, and 1 mM. The wild-type Na^+,K^+-ATPase equilibrated with 100 μM K^+ (Figure 5A) exhibited a slow phase reflecting the release of occluded K^+ and a rapid phase corresponding to phosphorylation of the enzyme fraction that does not contain occluded K^+. The slow and rapid phases constitute approximately 50% each, indicating that half of the wild-type enzyme was accumulated in the occluded $E_2(K_2)$ form at this K^+ concentration, in good agreement with the $K_{0.5}$ value for K^+ occlusion of 50−230 μM determined by fluorescence measurements on purified kidney enzyme (*44*, *45*). Under similar conditions, the Phe788 → Leu mutant exhibited almost no rapid phase of phosphorylation (98% slow phase), indicating that the K^+ occlusion sites of the mutant were almost saturated, and the rate constant characterizing the slow phase of phosphorylation, corresponding to release of occluded K^+, was 6−7 times lower in the mutant compared with the wild-type enzyme.

The extents of the slow and rapid phases depend on the concentration of K^+ and the apparent affinity of the K^+ occlusion sites. Following equilibration with a higher K^+ concentration of 1 mM, the extent of the slow phase of phosphorylation increased to as much as 93% in the wild-type and to 100% in the mutant (Figure 5B). As further seen in Figure 5A, even at a K^+ concentration as low as 10 μM, the extent of the slow phase remained higher than 90% in the mutant. This suggests that the apparent affinity of the K^+ occlusion sites is as much as 100-fold higher in the mutant relative to the wild-type. Because of the presence of contaminant K^+ in the membrane preparation and buffer media, it was impossible to reduce the K^+ concentration in the equilibration mixture much further. Hence, to examine whether the Phe788 → Leu mutant was able to display a rapid phase of phosphorylation similar to that corresponding to the nonoccluded fraction of the wild-type enzyme, Na^+ was added to the equilibration mixture to compete with K^+. As shown in Figure 6, in the presence of 100 mM Na^+, the fraction of mutant enzyme accumulated in the slowly phosphorylating form was 5, 53, and 81% at 10 μM, 100 μM, and 1 mM K^+, respectively. Thus, at this high Na^+ concentration, the apparent affinity of the K^+ occlusion sites in the mutant is similar to the affinity observed for the wild-type in the absence of Na^+ (cf. Figure 5A). Note also that following equilibration with K^+ in the presence of 100 mM Na^+, the rate constant reflecting the release of K^+ in the mutant was enhanced 4−5-fold relative to the value determined without Na^+ in the equilibration mixture. For the wild-type enzyme, 100 mM Na^+ completely prevented K^+ occlusion at a K^+ concentration of 100 μM.

K^+ Independent Dephosphorylation. In the wild-type Na^+,K^+-ATPase, the steady-state phosphorylation level measured at a Na^+ concentration of 150 mM in the absence of K^+ amounts to at least 75% of the maximal phosphorylation level determined in the presence of oligomycin to stabilize the phosphoenzyme. By contrast, the steady-state phosphorylation level in the Phe788 → Leu mutant constituted only 30−35% of the level of oligomycin-supported phosphorylation (data not shown). Because the mutant was able to hydrolyze ATP at a high rate in the presence of Na^+ without K^+ (Figure 1), a possible explanation of the low steady-state phosphorylation level would be an increased rate of K^+-independent dephosphorylation, assuming the phosphoenzyme to be an intermediate in the Na^+-ATPase reaction cycle. To investigate this hypothesis, a series of dephosphorylation experiments was carried out. In all cases, the enzyme was phosphorylated with [γ-^{32}P]ATP in the presence of a Na^+ concentration of 20 mM that saturates the internal sites, and dephosphorylation was monitored upon a 10-fold dilution into a medium containing nonradioactive ATP together with Na^+ to produce final Na^+ concentrations ranging between 2 and 200 mM, or K^+ to produce a saturating K^+ concentration of 20 mM for comparison. As seen in Figure 7, the data could be fitted to monoexponential decays. At 2 mM Na^+, the dephosphorylation rate of the mutant was 8-fold that of the wild-type. The rate of dephosphorylation increased with increasing Na^+ concentration and the Na^+ concentration giving half-maximum activation of dephosphorylation was significantly lower in the mutant relative to the wild-type. In the mutant, the maximal rate of Na^+-induced dephosphorylation observed at 137 mM Na^+ amounted to 61% of the rate of K^+-induced dephosphorylation. Hence, the high Na^+-ATPase activity of the mutant can be accounted for by an increased ability to dephosphorylate in the absence of K^+.

K^+-Induced Dephosphorylation. In the wild-type Na^+,K^+-ATPase, potassium ions can enter the occlusion sites from either side of the membrane. During equilibration with K^+ in the experiments corresponding to Figure 5, K^+ binds to the unphosphorylated wild-type enzyme at intracellularly facing sites of low affinity inducing a conformational change that occludes the ions in the $E_2(K_2)$ form [the *direct* route (*2*)]. In the normal forward running mode of the enzyme cycle, K^+ binds with high affinity at the extracellularly facing sites of the phosphorylated E_2P form of the pump and induces dephosphorylation accompanied by K^+ occlusion [the *physiological* route (*2*)]. To examine the apparent affinity for K^+ at the external sites on the E_2P intermediate, the K^+ dependence of the dephosphorylation rate was determined as described previously for other mutants (*11*, *37*). Following phosphorylation by ATP in the presence of 20 mM Na^+ without K^+, various concentrations of K^+ were added and the initial rate of dephosphorylation was measured in each case. As seen in Figure 8, the Phe788 → Leu mutant displayed a rather high rate of K^+-independent dephosphorylation in accordance with the data in Figure 7, but the dephosphorylation rate increased further with increasing K^+ concentration. The apparent affinity for activating K^+ is 2−3-fold higher in the mutant compared with the wild-type enzyme, whereas the maximum dephosphorylation rates obtained at saturating K^+ concentrations are almost identical in the mutant and the wild-type enzyme.

Ouabain Sensitivity. Figure 9 shows the dependence on ouabain concentration of the Na^+,K^+-ATPase activity measured at 130 mM Na^+, 20 mM K^+, and 3 mM ATP in the wild-type and mutant enzyme preparations. Either enzyme

preparation contains in addition to the expressed exogenous enzyme also the endogenous COS cell Na^+,K^+-ATPase, and both data sets were fitted to a function with the ouabain-inhibited enzyme represented by the sum of two hyperbolic components, one representing the endogenous COS cell Na^+,K^+-ATPase ($K_{0.5}$ for ouabain inhibition 0.3 μM in this condition, see ref *9*) and the other, with low affinity, representing the expressed exogenous enzyme (either wild-type or mutant). In the wild-type enzyme preparation, the low-affinity component contributed by the exogenous enzyme activity constituted 88% of the total Na^+,K^+-ATPase activity, whereas the high-affinity component, corresponding to endogenous enzyme, constituted only 12%. Due to the very low turnover number of the mutant enzyme in the presence of 20 mM K^+ (cf. Figure 1), the relative contribution to the enzyme activity by the small amount of endogenous enzyme was higher in the mutant enzyme preparation (62%), with the low-affinity component contributed by the exogenous mutant enzyme activity constituting only 38%. Thus, the two components of the ouabain curve corresponding to the mutant enzyme preparation (mutant and endogenous enzyme) represent enzymes with very different turnover numbers, whereas in the wild-type enzyme preparation, the two components (wild-type and endogenous enzyme) represent enzymes with similar turnover numbers. On the basis of the turnover numbers of 932, 8500, and 8500 min^{-1} for the mutant, wild-type, and endogenous enzyme, respectively, at 130 mM Na^+ and 20 mM K^+ (Figure 1), and the fractional activities in Figure 9, it can be calculated that the mutant contributes 85%

$$\left(\frac{\frac{38}{932}}{\frac{38}{932} + \frac{62}{8500}} \times 100\% \right)$$

of the Na^+,K^+-ATPase molecules in the enzyme preparation, whereas the corresponding number for the wild-type is 88%. These expression levels are in accordance with the phosphorylation capacities of the preparations determined with and without preincubation with ouabain (see "Expression").

With respect to the ouabain affinity of the Phe788 → Leu mutant, it is noteworthy that the titration curve corresponding to the mutant crosses that of the wild-type, indicating a lower apparent affinity of the mutant compared with the wild-type ($K_{0.5}$ values of 807 and 106 μM, respectively). Because of the ouabain-K^+ antagonism, the lower apparent ouabain affinity of the mutant may be explained by the high K^+ affinity and stabilization of the $E_2(K_2)$ form of the mutant demonstrated above.

DISCUSSION

In the normal Na^+,K^+-ATPase reaction cycle of the wild-type enzyme, Na^+ at the internal transport sites and K^+ at the external transport sites activate ATP hydrolysis, whereas K^+ at the internal sites or Na^+ at the external sites inhibits the activity. Because of the large difference between the apparent Na^+:K^+ affinity ratios (Na^+:K^+ selectivities) on the two sides of the system, it is possible, even with broken membranes, to measure the activating effect of Na^+ on the cytoplasmic sites with the external sites saturated with K^+ and to measure the activating effect of K^+ on the external sites with the cytoplasmic sites saturated with Na^+ (*3*, *39*).

As revealed in Figures 1 and 2, the cation dependency of the overall rate of ATP hydrolysis shows several unique features in the Phe788 → Leu mutant. The inhibition of ATP hydrolysis by micromolar concentrations of K^+ in the presence of millimolar ATP has not been previously reported for any mutant Na^+,K^+-ATPase. This inhibition is counteracted by Na^+ in high concentrations, and in the total absence of K^+ the mutant catalyzes Na^+-activated ATP hydrolysis ("Na^+-ATPase activity") at an extraordinary high rate corresponding to 86% of the maximal Na^+,K^+-ATPase activity. Thus, in the mutant, the roles of Na^+ and K^+ appear to have been swapped to some extent, and the sidedness of the cation effects is less straightforward to distinguish in the mutant than in the wild-type.

K^+ Occluded $E_2(K_2)$ Form is Unusually Stable in the Phe788→Leu Mutant. The inhibition of the ATPase activity of the Phe788 → Leu mutant by low concentrations of K^+ in the presence of millimolar ATP is reminiscent of the behavior of the wild-type enzyme at submicromolar ATP concentrations, where the $E_2(K_2) \rightarrow E_1$ transition is very slow (*1*, *4*, *5*). The analysis of the partial reaction steps points to an unusual stability of the K^+-occluded $E_2(K_2)$ form as the cause of the inhibitory effect of K^+ on ATP hydrolysis in the Phe788 → Leu mutant. When $E_2(K_2)$ was formed by K^+ binding to unphosphorylated enzyme in the absence of ATP, the $K_{0.5}$ for K^+ occlusion was close to 1 μM in the mutant versus 100 μM in the wild-type. It is likely that in the absence of ATP, K^+ becomes occluded by binding at the cytoplasmically facing transport sites on E_1 in competition with Na^+ followed by a spontaneous E_1K_2 to $E_2(K_2)$ conformational change [the *direct* route (*2*)]. In the presence of 100 mM Na^+ to compete with K^+ binding, the $K_{0.5}$ for K^+ occlusion in the mutant was found to be 100 μM, i.e., similar to that determined for the wild-type in the absence of Na^+ and 100-fold lower than the $K_{0.5}$ of approximately 10 mM of the wild-type in the presence of 100 mM Na^+ (*44*, *45*). Thus, it appears that in the absence of ATP the mutation has changed the apparent Na^+:K^+ affinity ratio on the cytoplasmic side of the system about 100-fold in favor of K^+, thereby impairing the Na^+ selectivity dramatically. At least part of this effect may be ascribed to a decrease in the rate of the $E_2(K_2) \rightarrow E_1$ transition, since this step was 6−7-fold slower in the mutant relative to the wild-type even under conditions where Na^+ and ATP [two components that tend to destabilize $E_2(K_2)$] had been added to observe phosphorylation (Figure 5).

Further evidence that the mutant is stabilized in the $E_2(K_2)$ form comes from the increased apparent affinity for K^+ in activation of the *p*NPPase reaction, which is believed to be catalyzed by $E_2(K_2)$ (*3*, *40*), and the finding that the molecular rate of *p*NPP hydrolysis in the mutant is similar to that of the wild-type even though the maximum rate of ATP hydrolysis in the mutant is only one-third that of the wild-type. Moreover, the 10−11-fold lower apparent ATP affinity of the mutant relative to the wild-type in the Na^+,K^+-ATPase assay with 250 μM K^+ present is indicative of an increased K^+-ATP antagonism compatible with stabilization of the mutant in the $E_2(K_2)$ form that exhibits low ATP affinity. Likewise, the reduced apparent affinity of the mutant for ouabain (Figure 9) can be explained by an increased K^+-

Scheme 2: Reaction Scheme Showing the Pathways Leading to Na^+-Activated ATP Hydrolysis ("Na^+-ATPase Activity") in the Absence of K^+[a]

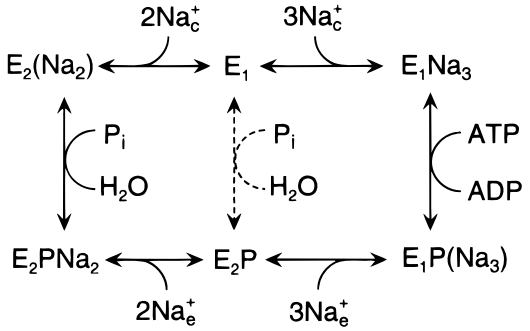

[a] The dephosphorylation route indicated by solid arrows corresponds to 3Na:2Na exchange while the dashed pathway corresponds to uncoupled Na^+ efflux.

ouabain antagonism due to stabilization of $E_2(K_2)$ (*46*). It is interesting that mutation of the equivalent phenylalanine, Phe786, of the ouabain-sensitive sheep α1 isoform[2] to isoleucine has been shown to reduce the apparent ouabain affinity 11-fold, thereby conferring ouabain resistance to HeLa cells expressing the mutant (*47*). Although the functional properties of the mutant were not further characterized in ref *47* and the ouabain affinities exhibited by the sheep wild-type and mutant Na^+,K^+-ATPases are 100-fold higher than those exhibited by the corresponding rat enzymes, it seems likely that the reduced apparent ouabain affinity of the sheep Na^+,K^+-ATPase mutant is caused by a mechanism similar to that presently proposed for the rat enzyme and not by a direct involvement of the phenylalanine in ouabain binding as suggested in ref *47*. This provides a compelling example of the caution needed when interpreting site-directed mutagenesis data in terms of selective interference with protein−ligand interactions at the ligand binding sites.

Phe788 → Leu Mutant Dephosphorylates at a High Rate in the Absence of K^+ at the External Sites. In the reaction cycle of the wild-type Na^+,K^+-ATPase, K^+ binding with high affinity at the extracellularly facing transport sites in the E_2P form is required for rapid dephosphorylation (Scheme 1). Therefore, only a low rate of ATP hydrolysis of maximally 6−10% of the maximum Na^+,K^+-ATPase activity can be observed in the mere presence of Na^+ without K^+. This "Na^+-ATPase activity" is usually ascribed to two different routes of slow dephosphorylation (Scheme 2, cf. refs *40* and *48*). Na^+ can bind with low affinity at the external "K^+ sites" and to some extent mimic K^+ by inducing dephosphorylation accompanied by transport of two Na^+ into the cells. In addition, E_2P without Na^+ bound may dephosphorylate slowly without accompanying Na^+ influx (dashed pathway in Scheme 2). The cycle obtained by combining the latter mode of dephosphorylation with the Na^+ efflux associated with phosphorylation and E_1P to E_2P transition (right limb of Scheme 2) gives rise to "uncoupled Na^+ efflux" (*40*).

In the Phe788 → Leu mutant, the Na^+-activated ATPase activity observed in the absence of K^+ was 3−4-fold higher than in the wild-type, and almost complete activation was obtained in the same range of Na^+ concentrations where the internal sites are filled ($K_{0.5}$ 2.3−2.5 mM). The high Na^+-ATPase activity displayed by the Phe788 → Leu mutant can be accounted for by the enhanced rate of K^+-independent dephosphorylation. Already at 2 mM Na^+, the dephosphorylation rate of the mutant was 8-fold higher than the rate determined for the wild-type, and the maximal rate of Na^+-induced dephosphorylation amounted to as much as 61% of the rate of K^+-induced dephosphorylation. Hence, the discrimination between Na^+ and K^+ on the extracellular side of the system is severely impaired in the mutant.

Previously, three other mutants with increased Na^+-ATPase activity have been characterized. In two of these mutants, Glu781 → Ala and Tyr773 → Leu, the replaced residue is located in transmembrane segment M5, and the third mutation, Asn326 → Leu, replaces a residue in M4 (*10*, *21*, *22*). In these mutants, the Na^+-ATPase activity continued to rise over a wide range of Na^+ concentrations up to 200 mM as in the wild-type. The low $K_{0.5}$ of 2.3 mM for activation of the major part of the Na^+-ATPase activity in the Phe788 → Leu mutant is thus unique and can in principle be explained by enhancement of the affinity for Na^+ at one or more of the external activating sites of the phosphoenzyme (the "K^+ sites"). Accordingly, the data in Figure 7 provide evidence for a significant decrease in the $K_{0.5}$ for Na^+ activation of dephosphorylation in the mutant relative to wild-type. However, since the apparent affinity is determined by a complex interplay between the intrinsic affinities of inhibitory and activating external sites and the rate constants for dephosphorylation of the various E_2P forms (*48*), the present data do not allow a definite conclusion as to whether any external site has indeed acquired higher intrinsic affinity in the mutant. Because of the high maximal rate of Na^+-induced dephosphorylation, the rate constant for dephosphorylation of at least one Na^+-bound E_2P form seems to be enhanced by the mutation, and because the dephosphorylation rate was increased 8-fold already at 2 mM Na^+, the rate constant for the Na^+-independent dephosphorylation associated with uncoupled Na^+ efflux (dashed pathway in Scheme 2) may also be enhanced. Since the latter pathway is inhibited by low concentrations of extracellular Na^+ in the wild-type (*40*, *48*), it is possible that the mechanism behind the mutational effect involves a disruption of the inhibitory site(s).

From Which Side of the Membrane Does the Inhibitory K^+ Enter the Occlusion Sites during ATP Hydrolysis? By titrating the K^+ dependence of dephosphorylation of E_2P, the apparent affinity for K^+ at the extracellularly facing sites was found to be only 2.6-fold higher in the mutant relative to the wild-type, a rather modest effect in comparison with the 100-fold increase in apparent affinity for K^+ being occluded in the dephosphoenzyme through the direct route. Moreover, the V_{max} for K^+-induced dephosphorylation was the same in the mutant as in the wild-type. Thus, it is clear that the inhibition by K^+ of progression of the ATPase cycle in the mutant does not result from stabilization of the E_2-PK_2 intermediate. However, during turnover of the enzyme in the presence of ATP, the inhibitory K^+ might enter the occlusion pocket by way of the external sites on the E_2P phosphoenzyme, i.e., by the physiological route (*2*). Following the dephosphorylation, the mutant enzyme would thus become arrested in the stable $E_2(K_2)$ form (*1*). Accordingly, the low-affinity activation by Na^+ of Na^+,K^+-ATPase activity in the mutant (Figure 1B) might be explained by competition between Na^+ and K^+ for activation of the dephosphorylation of E_2P, assuming that the Na^+-bound intermediate resulting

from Na^+-induced dephosphorylation ["$E_2(Na_2)$" cf. Scheme 2] is much less stable than its K^+-occluded counterpart resulting from the K^+-induced dephosphorylation.

The rudimentary activation of ATPase activity observed in the mutant at slightly lower K^+ concentrations than those causing inhibition, when the Na^+ concentration is increased to 200 mM (Figures 1 and 2), is a curious phenomenon which implies the existence of both activating and inhibitory K^+ sites of high affinity. It is possible that the K^+ activation is caused by the formation of a hybrid E_2PNa,K form having one sodium and one potassium ion bound at the two extracellularly facing transport sites instead of either two sodium or two potassium ions. The hybrid form of the phosphoenzyme might dephosphorylate as rapid as E_2PK_2, but the $E_2(Na,K)$ dephosphoform resulting from the dephosphorylation would differ from the $E_2(K_2)$ form by being less stable.

During ATP hydrolysis, the inhibitory K^+ might also enter the occlusion pocket by binding to one of the unphosphorylated intermediates in the cycle. The simplest possibility is that Na^+ and inhibitory K^+ compete for binding at the cytoplasmically facing transport sites in the E_1 form as envisioned for the nonturnover condition in the absence of ATP (see above). However, even in the presence of a K^+ concentration as high as 20 mM where the turnover rate is severely reduced in the mutant, the apparent affinity for Na^+ corresponding to the first activating phase in Figure 1B was found to be wild-type like. Therefore, it seems that under turnover conditions in the presence of millimolar ATP, K^+ is unable to compete efficiently with Na^+ at the cytoplasmically facing transport sites, a notion also gaining support from the fact that the cells expressing the mutant were able to survive in the presence of ouabain to inhibit the endogenous enzyme (see further below).

It is possible that one or more cation sites distinct from the transport sites are involved in the relief of the K^+ inhibition induced by high Na^+ concentrations. In line with the latter hypothesis, the presence of 100 mM Na^+ together with K^+ during formation of the K^+-occluded enzyme gave rise to a 4−5-fold enhancement of the rate of the $E_2(K_2)$ to the E_1 transition in the mutant (Figures 5 and 6). Previously, other workers have provided similar evidence for a simultaneous occupancy of transport and modifying sites (*49*, *50*).

How Can a Mutant with Such Abnormal Kinetics Sustain Cell Growth? The Phe788 → Leu mutant displays some of the most striking kinetic differences from wild-type yet seen in a functional Na^+,K^+-ATPase mutant, and one may ask how this can be compatible with cell growth in the presence of ouabain inhibiting the endogenous enzyme. The determination of site concentration by phosphorylation with and without preincubation with ouabain and the analysis of the biphasic ouabain dependence (Figure 9) demonstrate that the endogenous enzyme is not upregulated in the cells expressing the mutant. Under the conditions used for selection of stable transfectants the ouabain concentration is 5 μM and the endogenous enzyme is inhibited to such an extent that cells that do not express the exogenous enzyme die. Hence, the viability of the cells expressing the Phe788 → Leu mutant must be ascribed exclusively to the transport activity of the mutant enzyme. In the cell culture, the extracellular Na^+ and K^+ concentrations were kept at 155 and 2−5 mM, respectively, which seems to allow the extracellular sites to bind and transport K^+ rather than Na^+, as judged from the K^+ inhibition seen in Figure 2. The intracellular Na^+ and K^+ concentrations are unknown, and presumably the intracellular Na^+ concentration is higher than the normal 20−30 mM whereas the intracellular K^+ concentration may be lower than the normal 120 mM, due to the defective function of the mutant. Because, as discussed above, it seems that, under turnover conditions in the presence of millimolar ATP, K^+ is unable to compete efficiently with Na^+ at the cytoplasmically facing transport sites, it is reasonable to expect that these sites will be nearly saturated with Na^+ (cf. Figure 1). These considerations in conjunction with the data in Figures 1 and 2 lead to the conclusion that the turnover number of the mutant may be close to 1000 min^{-1} under the conditions prevailing in the cell culture. This is not a high value, but even the wild-type enzyme operates at a fraction of its maximal activity in the intact cell, so it is not unreasonable to assume that the activity of the mutant is sufficient to sustain cell growth.

What Is the Structural Basis for the Role of Phe788? The evidence from many functional studies suggests that the pathway for cation translocation in the Na^+,K^+-pump consists of a cation binding pocket common to Na^+ and K^+, which can open consecutively to either side of the membrane through access channels (*2*, *51*). Site-directed mutagenesis of the Na^+,K^+-ATPase has implicated residues with oxygen containing side chains in the transmembrane segments M4, M5, and M6 as part of a core region for cation binding and occlusion (*7*, *9*−*15*, *22*). Being located in M5, Phe788 may contribute to regulation of the structural properties of the transport pathway, and its role could be somewhat analogous to that of the aromatic residues conferring K^+ selectivity to the K^+ channels. In the K^+ channels, main-chain carbonyl oxygens are directed inward toward the pore, forming closely spaced ion binding sites within the selectivity filter. The aromatic residues of the selectivity filter interact with the network of aromatic amino acids surrounding the selectivity filter forming a massive sheet that may behave like a layer of springs holding the pore open at the proper diameter to confer ion selectivity on the basis of size (*34*). In the Na^+,K^+-ATPase, Phe788 might interact with some of the other aromatic residues present in the transmembrane domain to confer the appropriate selectivity properties by precise adjustment of the distance between the oxygen ligands in the cation coordination sphere and the spatial relationships that determine the dephosphorylation rates of the various E_2P forms through long-range effects between the cation-binding domain and the catalytic site.

A functional characteristic solely assigned to the Phe788 → Leu mutant, and not to any of the three other mutants known to exhibit high Na^+-ATPase activity (*10*, *21*, *22*), is an increased Na^+-ATPase activity at low Na^+ concentration in conjunction with an unusual stability of the K^+-occluded $E_2(K_2)$ intermediate. A tentative explanation of the difference between the Phe788 → Leu mutant and the other "Na^+-ATPase mutants" could be that in the Phe788 → Leu mutant the structure of the cation coordination sphere shrinks in the E_2 and E_2P forms due to disruption of the aromatic network. This might result in an increased affinity for the small Na^+ ion at the external sites and/or an enhanced efficiency of the signal transmission to the catalytic site that activates the dephosphorylation. A more compact

structure of the cation coordination sphere, with little flexibility left, might also explain the increased stability of the K^+-occluded $E_2(K_2)$ form.

ACKNOWLEDGMENT

I would like to thank Dr. Jens Peter Andersen for discussion and many helpful suggestions, Janne Petersen, Jytte Jørgensen, and Kirsten Lykke Pedersen for expert technical assistance, and Dr. R. J. Kaufman, Genetics Institute, Boston, MA, for the expression vector pMT2.

REFERENCES

1. Post, R. L., Hegyvary, C., and Kume, S. (1972) *J. Biol. Chem. 247*, 6530−6540.
2. Glynn, I. M. (1993) *J. Physiol. 462*, 1−30.
3. Skou, J. C. (1988) *Methods Enzymol. 156*, 1−25.
4. Skou, J. C., and Esmann M. (1980) *Biochim. Biophys. Acta 601*, 386−402.
5. Glynn, I. M., and Karlish, S. J. D. (1990) *Annu. Rev. Biochem. 59*, 171−205.
6. Lingrel, J. B., and Kuntzweiler, T. (1994) *J. Biol. Chem. 269*, 19659−19662.
7. Andersen, J. P., and Vilsen, B. (1995) *FEBS Lett. 359*, 101−106.
8. MacLennan, D. H., Rice, W. J., and Green, N. M. (1997), *J. Biol. Chem. 272*, 28815−28818.
9. Vilsen, B. (1993) *Biochemistry 32*, 13340−13349.
10. Vilsen, B. (1995) *Biochemistry 34*, 1455−1463.
11. Vilsen, B., and Andersen, J. P. (1998) *Biochemistry 37*, 10961−10971.
12. Nielsen, J. M., Pedersen, P. A., Karlish, S. J. D., and Jørgensen, P. L. (1998) *Biochemistry 37*, 1961−1968.
13. Pedersen, P. A., Nielsen, J. M., Rasmussen, J. H., and Jørgensen, P. L. (1998) *Biochemistry 37*, 17818−17827.
14. Jewell-Motz, E. A., and Lingrel, J. B. (1993) *Biochemistry 32*, 13523−13530.
15. Blostein, R., Wilczynska, A., Karlish, S. J. D., Argüello, J. M., and Lingrel, J. B. (1997) *J. Biol. Chem. 272*, 24987−24993.
16. Clarke, D. M., Loo, T. W., Inesi, G., and MacLennan, D. H. (1989) *Nature 339*, 476−478.
17. Vilsen, B., and Andersen, J. P. (1992) *J. Biol. Chem. 267*, 25739−25743.
18. Andersen, J. P., and Vilsen, B. (1994) *J. Biol. Chem. 269*, 15931−15936.
19. Hermsen, H. P. H., Swarts, H. G. P., Koenderink, J. B., and De Pont, J. J. H. H. M. (1999) *Biochim. Biophys. Acta 1416*, 251−257.
20. Ambesi, A., Dewitt, N. D., Petrov, V. V., Gupta, S. S., and Slayman, C. W. (1998) *Acta Physiol. Scand. 163* (Suppl. 643), 107−113.
21. Vilsen, B. (1995) *FEBS Lett.* 363, 179−183.
22. Vilsen, B., Ramlov, D., and Andersen J. P. (1997) *Ann. N. Y. Acad. Sci. 834*, 297−309.
23. Andersen, J. P. (1995) *J. Biol. Chem. 270*, 908−914.
24. Lutsenko, S., Anderko, R., and Kaplan, J. H. (1995) *Proc. Natl. Acad. Sci. U.S.A.* 92, 7936−7940.
25. Shin, J. M., Besancon, M., Simon, A., and Sachs, G. (1993) *Biochim. Biophys. Acta 1148*, 223−233.
26. Lutsenko, S., and Kaplan, J. H. (1995) *Biochemistry 34*, 15607−15613.
27. Béguin, P., Hasler, U., Beggah, A., Horisberger, J. D., and Geering, K. (1998) *J. Biol. Chem. 273*, 24921−24931.
28. Xie., Y., Langhans-Rajasekaran S. A., Bellovino, D., and Morimoto, T. (1996) *J. Biol. Chem. 271*, 2563−2573.
29. Bayle, D., Weeks, D., and Sachs, G. (1995) *J. Biol. Chem. 270*, 25678−25684.
30. Bamberg, K., and Sachs, G. (1994) *J. Biol. Chem. 269*, 16909−16919.
31. Dougherty, D. A. (1996) *Science 271*, 163−168.
32. Heginbotham, L., Abramson, T., and MacKinnon, R. (1992) *Science 258*, 1152−1155.
33. Silverman, S. K., Lester, H. A., and Dougherty, D. A. (1998) *Biophys. J. 75*, 1330−1339.
34. Doyle, D. A., Cabral, J. M., Pfuetzner, R. A., Kuo, A., Gulbis, J. M., Cohen, S. L., Chait, B. T., and MacKinnon, R. (1998) *Science 280*, 69−77.
35. Green, N. M. (1989) *Biochem. Soc. Trans. 17*, 970−972.
36. Møller, J. V., Juul, B., and le Maire, M. (1996) *Biochim. Biophys. Acta 1286*, 1−51.
37. Vilsen, B. (1997) *Biochemistry 36*, 13312−13324.
38. Esmann, M. (1988) *Methods Enzymol. 156*, 105−115.
39. Skou, J. C. (1957) *Biochim. Biophys. Acta 23*, 394−401.
40. Glynn, I. M. (1985) In *The Enzymes of Biological Membranes* (Martonosi, A. N., Ed.) Vol. 3, pp 35−114, Plenum Publishing Corp., New York.
41. Nørby, J. G., and Esmann, M. (1997) *J. Gen. Physiol. 109*, 555−570.
42. Drapeau, P., and Blostein, R. (1980) *J. Biol. Chem. 255*, 7827−7834.
43. Daly, S. E., Lane, L. K., and Blostein, R. (1996) *J. Biol. Chem. 271*, 23683−23689.
44. Karlish, S. J. D., and Yates, D. W. (1978) *Biochim. Biophys. Acta 527*, 115−130.
45. Karlish, S. J. D. (1980) *J. Bioenerg. Biomembr. 12*, 111−136.
46. Hansen, O. (1984) *Pharmacol. Rev. 36*, 143−163.
47. Palasis, M., Kuntzweiler, T. A., Argüello, J. M., and Lingrel, J. B. (1996) *J. Biol. Chem. 271*, 14176−14182.
48. Pedemonte, C. H. (1988) *J. Theor. Biol. 134*, 165−182.
49. Karlish, S. J. D., and Stein, W. D. (1985) *J. Physiol. (London) 359*, 119−149.
50. Forbush, B., III (1987) *J. Biol. Chem. 262*, 11104−11115.
51. Gadsby, D. C., Rakowski, R. F., and De Weer, P. (1993) *Science 260*, 100−103.

BI990951T